Article

Isotherm Models and First-Principles Studies of Gas Adsorption in Graphene Field-Effect Transistors: A Review

Chenrong Gong [1,2], Ran Wang [1,2], Jia Liu [3], Xianjie Wan [3], Zhou Yu [3], Weihua Liu [1,2] and Guohe Zhang [1,2,*]

[1] School of Microelectronics, Xi'an Jiaotong University, Xi'an, China
[2] The Key Lab of micro-nano electronics and system integration of xi'an city, Xi'an, China
[3] No.24 Institute, China Electronics Technology Group Corporation, Chongqing, China
* Correspondence: zhangguohe@xjtu.edu.cn; Tel.: +86-1377-210-2037 (F.L.)

Abstract: Graphene has attracted a lot of attention in gas sensing applications for its high surface area ratio and unique chemical or physical gas adsorption ability. Being an important research method, theoretical calculations play a key role in both illustrating the gas sensing mechanism of graphene and improving the gas sensing performance of graphene-based sensors. This review discusses the application of adsorption isotherm theory and first-principles studies to graphene gas sensors. Different isotherm theories are presented, including Langmuir, Freundlich, BET, and Temkin isotherm models, and it is illustrated how to investigate the adsorption information from them. The first-principles analysis of graphene-based gas sensors is presented. In general, doping with transition metals and nonmetals can improve the sensitivity of graphene to gases. This review shows the significance of using theoretical calculations to design novel and efficient gas sensors. The theoretical results obtained so far can be of great help in designing novel and efficient graphene-based gas sensors.

1. Introduction

Currently, there is an increasing concern for the environment, health, and industrial safety. Investigations on the detection and monitoring of toxic gases, volatile organic compound gases, and other harmful gases are of great significance. Sensors based on field-effect transistors (FETs) are of great attention in the field of gas detection because of their unique features of high sensitivity, small size, a small amount of sample required, easy handling, and low cost [1]. The current widely used silicon transistor-based sensors suffer from limitations such as low sensitivity and selectivity [2]. In recent years, research on the applications of low-dimensional materials (e.g., nanotubes, nanowires, and two-dimensional thin films) for sensors has been intensified to overcome the limitations of silicon [3-8].

Graphene (G) has been studied and developed as a gas-sensing material because of its ultrathin nature, extremely large surface-to-volume ratio, low electrical noise, and high carrier mobility [9-10]. The sensing ability of graphene can reach the molecule level [11-12]. In 2007, Schedin et al. demonstrated that graphene sensors can detect NO_2, NH_3, CO, and H_2O molecules at atmospheric pressure [13]. Subsequently, graphene-based sensors were widely exploited for detecting various types of gases, for example, NH_3, CO, O_2, NO_2, H_2, CH_4, SO_2, H_2S, and volatile organic compounds (VOCs) [12, 14-17].

Experimentally, the current conception of novel graphene sensor materials and the required performance improvements are largely limited by the lack of rapid and economical synthesis routes and post-testing strategies to ensure their functionality. Currently, different synthesis techniques such as chemical vapor deposition, sputtering, drop-casting, spin coating, and inkjet printing have been used to fabricate high-quality graphene for the detection of toxic gases [18-19]. However, many of these methods are expensive and not easily scalable for mass production. In addition, it is difficult to control the doping concentration and the number of graphene layers. Undoubtedly, such limitations can be overcome if sensor materials are designed, modeled, and evaluated from a theoretical point of view (e.g., first-principles methods). Compared to traditional experimental methods, theoretical calculations offer significant advantages, such as cost savings in terms of time and effort. In addition, computational methods can determine the atomic processes involved in gas sensing and explore the intrinsic changes within the sensing material. With the development of computational materials science, theoretical computational methods can be used not only to provide rational and insightful interpretations of experimental results but also to help design new material structures that lead to new functionalities.

This review focuses on the contribution of theoretical calculations (including isotherm models and first-principles studies) in the study of gas sensing properties of graphene field-effect transistors (GFETs). These theoretical results can provide some basis for the design of novel and efficient graphene-based gas sensors.

2. Working Principle of GFET Sensors

Many research groups are investigating field-effect transistors (FETs) using graphene as a channel [20]. Although its zero-band gap and low on/off current ratio hinder its application in digital and analog circuits. The bipolar property of graphene makes it suitable for FET sensors because the carrier density in graphene can be easily tuned by the gate voltage [11]. Compared to most commonly used chemical sensors, GFET sensors have the advantage of high selectivity and high sensitivity.

The mechanism of gas detection by GFET sensors is such that a change in the conductivity of the channel (graphene) is caused by an external electric field induced by electron donor (reduction) or electron acceptor (oxidation) type gas molecules. Figure 1 (a) shows the schematic of the most used back gated GFET sensor, which is composed of a back gate, a source, a drain, and a graphene channel. The typical drain current-gate voltage characteristics are shown in Figure 1 (b). Since both electrons and holes are available as majority carriers in pristine graphene, GFETs display an ambipolar characteristic. The Dirac point is also known as the 'charge neutrality point (CNP)'. The concentration of electrons and holes at this point is considered to be almost equal, with the lowest drain current. The oxidizing gas (depicted in Figure 1), as an electron acceptor, increases the hole density in the graphene channel, while the reducing gas (electron donor) decreases the same density. Thus, the oxidizing gas causes an increase in the hole current and a decrease in the electron current with respect to the pristine graphene. Reducing gases lead to the opposite phenomenon. In addition, a shift of the "Dirac point" (to the right/left in the case of oxidizing/reducing gases) was observed [21].
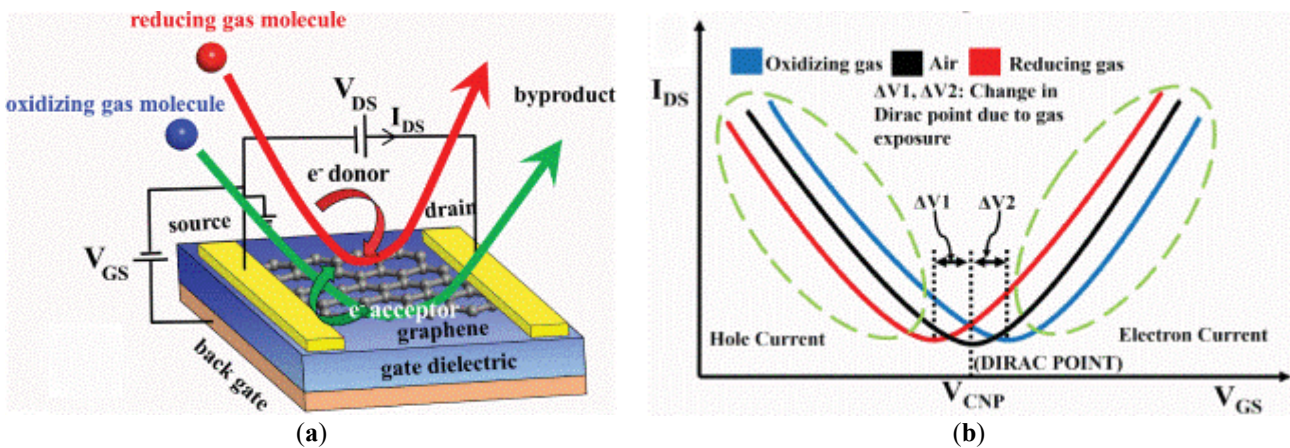

Figure 1. (a) Schematic representation of back gated GFET gas sensor device [24]. **(b)** Typical drain current-gate voltage characteristics [24]. © [2021] IEEE. Reprinted, with permission, from [IEEE Sensors Journal].

When the target gas is off, the simplified drain current (I_D) of the GFET sensor is expressed by [22]

$$I_D = \mu W/L\, C_{ox}\left(V_G - V_D/2\right)V_D \tag{1}$$

where μ is the carrier mobility, W and L are the width and length of the sensing layer, respectively, C_{ox} is the unity gate capacitance, V_D and V_G are the drain voltage and the gate voltage, respectively. When the sensing layer is exposed to the target gas and the modification of the graphene surface is taken into account in the above relationship, the following equation is obtained [23]:

$$I_D = \mu W/L\left[C_{ox}\left(V_G - V_D/2\right) + Q_m\right]V_D \tag{2}$$

here, $Q_m\left(\text{C.cm}^{-2}\right)$ is the interface charges induced by the gas molecules. Importantly, Q_m is not zero when electrons transfer between the gas molecules and graphene channel. This is the reason why the GFET sensor can detect the gas concentration when it reacts with an electron-donor or electron-acceptor gas. From Equation (2), we can see the synergistic effect: for a given sensing layer and drain voltage (V_D), I_D depends on not only the gate voltage (V_G) but also the adsorbed gas molecules (Q_m).

3. Adsorption isotherm models

Isotherm is the relationship between the concentration of adsorbent in the liquid phase and the amount of adsorption on the solid phase when the adsorption reaches equilibrium at a certain temperature [25]. Modeling adsorption data with an isotherm model is one of the most convenient and commonly used methods [26]. Isotherms can be used to model equilibrium adsorption data and to study adsorption information such as adsorption mechanism, maximum adsorption capacity, and adsorbent properties. In this section, four common adsorption isotherms and their application to GFET sensing of gases are described.

3.1. Langmuir Isotherm

During the study of the adsorption of gases on metals at low pressure, Langmuir found some regularities based on experimental data. Then he proposed an isothermal equation for adsorption based on the viewpoint of kinetics and summarized Langmuir adsorption theory of single-molecule layer [27]. The basic idea of this theory is that the adsorption of a gas on a solid surface is the result of a dynamic equilibrium between two opposing processes of gas adsorption and desorption on the surface of the adsorbent. This theory is based on the following assumptions: (1) the solid surface is homogeneous; (2) the adsorption is monolayer; (3) the adsorbed molecules do not interact with each other. Based on the above assumptions, the Langmuir adsorption isotherm can be derived from the adsorption kinetics.

The adsorption rate can be estimated using gas kinetic theory and is determined by several parameters: (1) the collision rate ϕ at the surface at a pressure P ($\phi = PN_A/(2\pi MRT)^{1/2}$, where N_A is the Avogadro constant, M is the molar mass of the gas, and R is the gas constant); (2) the surface area occupied by a single adsorbed particle (S); (3) the location available for adsorption ($1-\theta$); (4) the adhesion coefficient ($K = K_0 \exp(-E_A/RT)$). On the other hand, the desorption rate depends on the surface coverage θ and the average time of contact between the adsorbed particles and the surface $\tau = v^{-1}\exp(E_D/RT)$. Thus, the net adsorption rate of a certain gas on a solid surface can be expressed as the difference between the adsorption rate and the desorption rate [28]:

$$\frac{d\theta}{dt} = \frac{PN_A}{\sqrt{2\pi MRT}}S(1-\theta)K_0\exp(-\frac{E_A}{RT}) - v\theta\exp(-\frac{E_D}{RT}) \tag{3}$$

where E_A and E_D are the activation energies of adsorption and desorption, respectively. K_0 is the condensation coefficient and v is the oscillation frequency of the adsorbed particles. Surface coverage is defined as $\theta = N(t)/N_0$, $N(t)$ is the concentration of particles adsorbed on the solid surface at the time t, and N_0 is the concentration of total available adsorption sites. Integrating Equation (3) gives

$$\theta = \frac{N(t)}{N_0} = \frac{P}{P+b}(1-\exp(-K_1 t)) \tag{4}$$

with

$$K_1 = \frac{K_0 SPN_A}{\sqrt{2\pi MRT}}\exp(-\frac{E_A}{RT}) + v\exp(-\frac{E_D}{RT}) \tag{5}$$

$$b = \frac{v}{K_0 SN_A}\sqrt{2\pi MRT}\exp(\frac{E_A - E_D}{RT}) \equiv b_0\exp(-\frac{Q}{RT}) \tag{6}$$

where

$$b_0 = \frac{v}{K_0 SN_A}\sqrt{2\pi MRT} \tag{7}$$

Here $Q \equiv E_D - E_A > 0$ is the heat of adsorption. It can be seen from Equation (4) that $N(t)$ is a dimensionless parameter, and the magnitude of b (also including b_0) is the same as the pressure. The unit of K_1 is the same as the frequency. Therefore, if t_A is defined as the inverse of K_1, t_A has units of time. Then Equation (4) can be written as

$$\frac{N(t)}{N_0} = A(1-\exp(-K_1 t)) = A\left[1-\exp\left(-\frac{t}{t_A}\right)\right] \tag{8}$$

where $A = P/(P+b)$ is the response magnitude of the response rate. This equation has been used in a few articles to fit the adsorption process of gases.

The Langmuir adsorption isotherm can be obtained when the adsorption and desorption rates in Equation (4) are equal or $t \to \infty$ in Equation (4).

$$\frac{N(t)_{\text{equil}}}{N_0} = \frac{P}{P+b} \tag{9}$$

The desorption process starts with the escape of the adsorbed molecules on the surface to the gas phase. This is a very simple chemical process. For the occupied site concentration, θ_A,

$$-\frac{d\theta_A}{dt} = K_D \theta_A \tag{10}$$

The thermal dependence of K_D is based on the activation free energy E_D:

$$K_D = v \exp\left(-\frac{E_D}{RT}\right) = v \exp\left(-\frac{E_A + Q}{RT}\right) \tag{11}$$

The frequency v is in the normal range of molecular vibrations, which is about 10^{12} to 10^{13} s^{-1}. The solution of Equation (10) is

$$\theta_A = \theta_A(0) \exp\left(-K_D t\right) = \theta_A(0) \exp\left(-\frac{t}{t_D}\right) \tag{12}$$

where $\theta_A(0)$ is the initial concentration of the occupied sites in the desorption process, $t_D \equiv 1/K_D$.

The adsorption of a few gases on the GFET can be explained by the Langmuir model. In 2012, Madhav Gautam et al. [29] used the back-gated GFET to study the sensing of ammonia (NH_3) in ppm levels. The Langmuir method was used to estimate the moving rate of the Dirac peak, indicating that the rate increases linearly with temperature. The dependence of the temporal responses on the oxygen concentration can be well approximated by the Langmuir law [30-31]. The adsorption of other gases (e.g., NO_2 [32-33], H_2 [34-35]) on the GFET can also be approximated by Langmuir isotherm.

3.2. Freundlich Isotherm

The Langmuir model is based on the ideal situation, however, the surface energy of the solid is inhomogeneous due to the presence of polycrystalline structure and surface defects. Therefore, most of the experimental results cannot be accurately explained by Langmuir isotherm. Then some other isotherms have been proposed based on this. Freundlich Isotherm is an empirical equation.

Based on experiments, it has been proposed that the activation energy for adsorption and desorption during inhomogeneous adsorption is logarithmically related to θ [36]

$$E_A = E_A^0 + \beta \ln \theta \tag{13}$$

$$E_D = E_D^0 - \gamma \ln \theta \tag{14}$$

The adsorption heat Q is

$$Q = E_D - E_A = \left(E_D^0 - E_A^0\right) - \left(\beta + \gamma\right) \ln \theta = Q^0 - \alpha \ln \theta \tag{15}$$

Substituting Equations (13) and (14) into Equation (3) yields the net adsorption rate on non-uniform surfaces:

$$\frac{d\theta}{dt} = k_A P \theta^{-\frac{\beta}{RT}} - k_D \theta^{\frac{\gamma}{RT}} \tag{16}$$

Since θ varying between 0 and 1, the effect of $1-\theta$ and θ is negligible compared to $\theta^{-\frac{\beta}{RT}}$ and $\theta^{\frac{\gamma}{RT}}$ in the case of little or moderate coverage, which is accounted for in the constant term. In the above equation

$$k_A = \frac{N_0 \exp\left(-\dfrac{E_a^0}{RT}\right)}{\sqrt{2\pi MRT}} S(1-\theta) \tag{17}$$

$$k_D = \nu\theta \exp\left(-\frac{E_d^0}{RT}\right) \tag{18}$$

When the adsorption rate is equal to the desorption rate, the Freundlich Isotherm is obtained [28, 37-38]:

$$\frac{N(t)_{\text{equil}}}{N_0} = kP^{1/n} \tag{19}$$

where $k = \left(\dfrac{k_a}{k_d}\right)^{\frac{RT}{\alpha}}, n = \dfrac{\alpha}{RT}$.

    However, this model cannot predict the surface coverage at infinite pressure. This deficiency can be corrected by the following expression [28, 38]:

$$\frac{N(t)_{\text{equil}}}{N_0} = \frac{kP^{1/n}}{1+kP^{1/n}} \tag{20}$$

When the gas concentration is very low, the value tends to $kP^{1/n}$, and when the pressure tends to infinity, the value tends to 1. In some articles, Equation (15) is also written in the following form [28, 37]:

$$\frac{N(t)_{\text{equil}}}{N_0} = \frac{\alpha C^\beta}{1+\alpha C^\beta} \tag{21}$$

where C is the concentration of the target gas. Thus, the gas adsorption process can be explained by the following expression

$$\frac{N(t)}{N_0} = \frac{\alpha C^\beta}{1+\alpha C^\beta}\left(1-\exp\left(-\frac{t}{t_A}\right)\right) \tag{22}$$

    In practical applications, the experimental data are fitted using $R_{res}(t) = A\left(1-\exp\left(-\dfrac{t}{t_A}\right)\right)$ and $R_{rec}(t) = B\left(\exp\left(-\dfrac{t}{t_D}\right)\right)$.

Here, $R_{res}(t)$ is for the response and $R_{rec}(t)$ is for the recovery of the device. A, B are the amplitudes and t_A, t_D are the time constants for response and recovery, respectively. In 2012, Madhav Gautam et al. reported the ammonia sensing behavior of graphene films decorated with platinum nanoparticles [37] and gold nanoparticles [39], respectively. The effect of surface inhomogeneity was analyzed using the Freundlich isotherm. In 2018, Tao Xu et al. [40] analyzed hydrogen adsorption on surfactant-modified graphene using the Freundlich isothermal adsorption model.

    In addition to the direct use of Freundlich Isotherm to fit the gas adsorption process on GFETs, the heat of adsorption (Q) and activation energy (E_A) were further estimated from the kinetic data in several studies [28, 37]. According to the Langmuir model and Freundlich model, it is assumed that

$$Z \equiv \frac{A}{1-A} = \left(\frac{1}{b}\right)C = \alpha C^\beta \tag{23}$$

Then

$$\frac{1}{b} = \frac{dZ}{dC} = (\alpha\beta)C^{\beta-1} \tag{24}$$

Substituting this into Equation (6) gives:

$$b = \left(\frac{1}{\alpha\beta}\right)C^{1-\beta} = b_0 \exp\left(-\frac{Q}{RT}\right) \tag{25}$$

$$Q = RT\left(\ln b_0 - \ln b\right) = RT\left[\ln b_0 + \ln\left(\alpha\beta\right) - \left(1-\beta\right)\ln C\right] \qquad (26)$$

Then, for a given concentration of the target gas at a given temperature, if we know the value of b_0, we can determine the heat of adsorption (Q).

For low concentration of target gas (in ppm level), the ratio of P and b_0, P/b_0, is extremely small and its contribution to the time constant is negligible [28, 39]. In this approximation, time constants can be expressed as

$$t_D = v^{-1}\exp\left(\frac{E_A + Q}{RT}\right) \qquad (27)$$

A plot of the time constant of the device during the reaction as a function of the target gas concentration was fitted with $t = aC^{-b}$, where a and b are the fitted parameters. If we consider t to be the effective time constant of the device at a given temperature, Equation (27) can be rewritten as:

$$aC^{-b} = v^{-1}\exp\left(\frac{E_A + Q}{RT}\right) \qquad (28)$$

Then activation energy can be calculated as

$$E_A = RT\ln\left(\frac{av}{C^b}\right) - Q \qquad (29)$$

Table 1 lists some studies using Freundlich Isotherm to estimate the heat of adsorption and activation energy of gas adsorption on GFETs, which is a direction where research can be initiated later.

Table 1. The activation energy of adsorption E_A (eV) and heat of adsorption Q (eV) of gases on graphene film for different concentrations at different temperatures.

Material	Gas	T (K)	C(ppm)	*Q* (eV)	*Ea* (eV)	Reference
Pt-decorated graphene	NH$_3$	298	15	0.0402	0.0353	[37]
			31	0.0396	0.0352	
			48	0.0393	0.0351	
			58	0.0392	0.0350	
		323	15	0.0462	0.0352	
			31	0.0460	0.0353	
			48	0.0458	0.0353	
			58	0.0458	0.0353	
		348	15	0.0502	0.0358	
			31	0.0498	0.0353	
			48	0.0496	0.0351	
			58	0.0495	0.0350	
		373	15	0.0540	0.0362	
			31	0.0538	0.0354	
			48	0.0537	0.0350	
			58	0.0537	0.0348	
Gold nanoparticles-decorated graphene	NH$_3$	Room temperature	15	0.0413	0.0383	[39]
			31	0.0409	0.0386	
			48	0.0407	0.0387	

58	0.0406	0.0388

3.3. Brunauer - Emmett -Teller (BET) Isotherm

The multilayer adsorption isotherm, known as BET isotherm, is a theory of physical adsorption on a solid surface，which was proposed by Stephen Brunauer, Paul Emmett, and Edward Teller in 1938 [41]. It is based on the Langmuir adsorption isotherm with the following basic assumptions: (1) the adsorbent surface is homogeneous; (2) there is no interaction between adsorbed molecules; (3) adsorption can be a multi-molecular layer, and it is not necessary to completely cover a single layer before laying other layers; (4) the first layer of adsorption is the direct interaction between the gas molecules and the solid surface, and the heat of adsorption is different from the heat of adsorption of the subsequent layers; while the second and subsequent layers are the interaction between the same gas molecules, and the heat of adsorption of each layer is the same, which is the heat of liquefaction of the adsorbed mass.

The BET adsorption equation is:

$$V = V_m \frac{Cp}{(p_s - p)\left[1 + (C-1)\frac{p}{p_s}\right]}$$ (30)

where V represents the amount of adsorption at equilibrium pressure p, V_m represents the volume of gas required to spread a single layer of molecules on the solid surface, p_s is the saturation vapor pressure of the gas at the experimental temperature, and C is a constant related to adsorption, $\frac{p}{p_s}$ called the specific pressure of adsorption.

The BET formula is mainly applied to determine the specific surface of a solid (i.e., the surface area of 1 g of adsorbent). It is usually applied only for specific pressures ($\frac{p}{p_s}$) in the range of about 0.05 to 0.35, which is because this formula is based on the assumption that it is multilayer physisorption. There are many methods to determine the specific surface, but BET adsorption isotherm is the most widely used method in the industry and has the most reliable test results. Almost all domestic and international standards are established based on BET adsorption isotherm.

For GFET gas sensors, the BET model can be used to calibrate the surface area. Othman et al. determined the specific surface area by exploiting the BET model in the relative pressure range between 0.05 to 0.20 of glucose-derived graphene [42]. The surface areas of graphene sheets decorated with Fe nanoclusters were determined from the nitrogen adsorption isotherm employing the BET method [43].

3.4. Temkin Isotherm

Based on experiments, it has been proposed that the activation energy of adsorption increases linearly with θ and the activation energy of desorption decreases linearly with θ during inhomogeneous adsorption at medium coverage,

$$E_A = E_A^0 + \beta\theta$$ (31)

$$E_D = E_D^0 - \gamma\theta$$ (32)

where E_A^0 and E_D^0 is equivalent to the activation energy of adsorption and desorption at $\theta = 0$, and β, γ are constants. The adsorption heat Q is

$$Q = E_D - E_A = (E_D^0 - E_A^0) - (\beta + \gamma)\theta = Q^0 - \alpha \ln\theta$$ (33)

Substituting Equations (31) and (32) into Equation (3) yields the net adsorption rate on non-uniform surfaces:

$$\frac{d\theta}{dt} = k_A P \exp\left(-\frac{\beta\theta}{RT}\right) - k_D \exp\left(\frac{\gamma\theta}{RT}\right)$$ (34)

When equilibrium is reached at a constant temperature, Temkin Isotherm can be derived:

$$\theta = \frac{RT}{\alpha} \ln(A_0 p)$$ (35)

where A_0 is a constant. It represents the relationship between p and the equilibrium coverage at moderate coverage, characterized by θ linear relationship with $\ln p$.

However, no studies were available on the application of Temkin isotherm to graphene gas sensors.

Of the several isotherms mentioned above, the BET isotherm is only applicable to multilayer physisorption. For the Langmuir and Freundlich isotherm, it can be used for either physisorption or chemisorption. In contrast, the Temkin isotherm can only be used for the chemisorption of a single layer. It may be because in chemisorption the particles must be adsorbed on the adsorption centers that can form bonds, whereas in physical adsorption there is no such limitation and they can be adsorbed on any position on the surface, so the coverage of physical adsorption is much larger than that of chemisorption.

4. First-principles studies

The first principles or ab initio methods are based on the quantum mechanics theory. Specifically, the density functional theory (DFT) is a method to study the electronic structure of multi-electron systems utilizing electron density, expressed in terms of the electronic density distribution [44]. The DFT-based simulations are essential for understanding and explaining the experimental results at the molecular level. The gas-sensing performance of novel materials can be theoretically predicted with the help of DFT calculations [45]. The DFT calculations provide important information, such as the possible adsorption configurations, the preferred adsorption sites, the adsorption energy, electron transfer, electronic and transport changes after gas adsorption, and possible methods to enhance adsorption or desorption, that are critical for designing novel gas sensors [46]. With the critical role of these theoretical calculations in the design of gas sensors, numerous DFT studies have been conducted to investigate novel graphene-based gas sensors. This section provides a detailed analysis of the progress of graphene-based gas sensors through a first-principles approach.

4.1. Pristine Graphene

There have been some theoretical studies of pristine graphene gas sensors [47-50]. Leenaerts et al. investigated the adsorption of H_2O, NH_3, CO, NO_2, and NO on pristine graphene [47]. They used a 4×4 graphene supercell to investigate the adsorption of a single molecule onto it using the generalized gradient approximation (GGA); the adsorption energies of -47, -31, -14, -67, and -29 meV were found for H_2O, NH_3, CO, NO_2, and NO molecules, respectively [47]. At the same time, Wehling et al. conducted the first joint experimental and theoretical investigation of the NO_2 adsorption on graphene [49]. They used the local density approximation (LDA) and GGA for their calculations [49]. Lin et al. studied the adsorption behavior of H_2O, NH_3, CO, and NO_2 on graphene with the van der Waals density functional (vdW-DF2) and LDA methods adopting with the projected augmented wave (PAW) method [48]. Silvestrelli et al. applied the van der Waals-Quantum Harmonic Oscillator-Wannier function (vdW-QHO-WF) method to study the weak interactions of atoms and small molecules with ideal planar graphene surface [50]. They compared the results to those obtained by other DFT vdW-corrected schemes and found that an accurate description of the X-graphene interaction requires a proper treatment of many-body contributions and short-range screening effects [50]. It is shown that although the adsorption energy of the gas on graphene is significantly affected by the method used, the interaction between the gas and the pristine graphene is weak. This could limit the sensitivity of pristine graphene for gas detection.

4.2. Doped Graphene

To improve the reactivity of pristine graphene gas detection, researchers have employed different strategies. Doping is one of the most frequently used methods to modify the properties of graphene. So far, there have been numerous DFT studies on gas adsorption on doped graphene. It has been reported that the doping of both transition-metal [51-56] (Co, Pt, Pd, Ni, Cu, Ag, etc.) and nonmetal [57-59] (B, N, P, Cl, etc.) elements can change the electronic properties and chemical activity of graphene, as shown in Table 2.

According to theoretical calculations, with large binding energy to the surrounding atoms, the dopants can always occupy vacancies [60]. Moreover, strong orbital hybridization between the dopant and the gas molecule can promote electron transfer, hence greatly improving the sensitivity of the graphene [61]. Calculations of optimized geometries, adsorption energies, density of states, and charge transfer analysis show that most gas molecules are precipitated on the doped substrate by chemisorption instead of by weak physisorption, which is dominant on the pristine surface [45]. Among the gases reviewed, CO gas is the most investigated due to its high toxicity in humans [62]. It is also observed that the GGA (specifically PBE) method is the most widely used approach used for studying doped graphene for use in gas sensors. Although all calculations are conducted at the DFT level, there are discrepancies between the results reported in Table 1. These can be attributed to various factors, such as the functional and dispersion corrections employed in the calculations, the type and site of gas adsorption on which the adsorption energy was calculated, among others.

Decorating graphene with transition metal can significantly expand the interactions between gas molecules and graphene, where the adsorption energy is much higher than that of pristine graphene (See Table 1). Such increments in the adsorption energy can be attributed to the modification of the electronic properties of transition metals-decorated graphene compared to undecorated pristine graphene. Particularly, for the detection of NO_2 molecules, Pt- and Ni-decorated graphene is of high sensitivity, while for the detection of H_2S molecules, Pt-decorated graphene is more desirable [54]. Li-decorated boron-doped graphene has more significant adsorption energy to NO than that of Li-decorated pristine graphene because of the chemical interaction of the NO gas molecule [55]. Kumar et al. investigated the adsorption properties of CO, NH_3, CH_4, SO_2, and H_2S molecules over niobium doped graphene sheet (Nb/G) and found that CO and SO_2 molecules showed chemisorption on Nb/G, while NH_3, CH_4, and H_2S showed physisorption on Nb/G [63]. Chen et al. found that Ti and V dopant atoms can significantly enhance the interaction between H_2CO molecules and graphene [64]. Based on the first-principles calculations, Tang et al. comparably investigated the sensing performances of Fe embedded graphene sheets (including monolayer Fe-MG and bilayer Fe-BG) toward toxic gases (NO, CO, HCN, and SO_2), and found that the increased layer of graphene substrate can be utilized as a good sensor for toxic gas molecules, yet the metal Pt supported substrate can enhance the magnetic property of adsorbed gas on the Fe-graphene systems [65]. Jia et al. investigated the adsorption performance of NO/NO_2 molecules on intrinsic, Ag-doped, Au-doped, and Pt-doped graphene with the first-principles method based on density functional theory [66]. The results showed that the adsorption energy of Ag/Au/ Pt -doped graphene for NO/NO_2 molecules is larger than that of intrinsic graphene, and the charge densities of doped graphene and NO/NO_2 molecules overlap effectively.

Another approach widely used to modify the reactivity of pristine graphene is through doping nonmetal. Dai et al. conducted a theoretical study of the adsorption of several common gas molecules on B-, N-, Al- and S-doped graphene using DFT and found that only NO_2 binds to S-doped graphene, only NO and NO_2 bind to B-doped graphene, while Al-doped graphene is much more reactive and can bind more gases [59]. Then they conducted a theoretical study of the adsorption of gas molecules on P-doped graphene (PG) using density functional theory revealing that H_2, H_2O, CO_2, CO, N_2, and NH_3 molecules are physically adsorbed, while NO, NO_2, SO_2, and O_2 molecules are strongly chemisorbed on PG by forming P-X (X = O, N, S) bonds [67]. Zhang et al. found the transport behavior of a gas sensor using B-doped graphene shows a sensitivity two orders of magnitude higher than that of pristine graphene [58]. After analyzing the adsorption behaviors of methane adsorbed on different graphenes (pristine, and B-, N-, P-, and Al-doped monolayer and multilayer) using density-functional theory, Chen et al. found monolayer Al-G is the optimal molecular structure for CH_4 gas sensing application [57]. By investigating the effect of doping Ti or N atoms on the interaction of the CO, NO, SO_2, and HCHO with graphene through density functional theory calculations, Zhang et al. found that the Ti-doped graphene sheet demonstrated selective gas absorption, which implied that the Ti-doped graphene sheet is more effective than the N-doped graphene sheet in detecting and removing gas molecules [68]. Later they found out that the interactions between gases (NO_2, NO, and O_2) and Ti- or N-doped graphenes are not affected by the size of graphene [69]. Li et al. theoretically studied the adsorption of SO_2 on intrinsic graphene and heteroatom-doped (B, N, Al, Si, Cr, Mn, Ag, Au, and Pt) graphene samples with a first-principles approach based on DFT [70]. The Cr and Mn were found to be probably the best choices among all dopants.

Table 2. Adsorption energies of gases on doped graphene.

Materials	Elements	Gas	Ea(eV)	Method	Reference
Graphene	Co	NO	-4.04	PBE	[51]
		SO_2	-2.35		
		NH_3	-1.46		
		CO	-2.19		
		HCN	-2.14		
Graphene	Pt	NO	-2.06	B3LYP	[52]
Graphene	Pt	SO_2	-1.08	B3LYP	[53]
		O_3	-2.04		
Graphene	Ni, Pd, Pt	NO_2	-2.40, -1.59, -2.00	PBE	[54]
		H_2S	-1.81, -1.22, -2.03		
Graphene	Ti, V	H_2CO	-1.12, -1.94	PBE	[64]
Graphene	Pd	CO	-0.91	PBE	[56]
		NO	-3.92		
Graphene	Fe	NO	-2.40	PBE	[65]
		CO	-1.71		
		HCN	-1.67		

		SO$_2$	-1.68		
Graphene	Li, B	CO	-0.55, -0.51	B3LYP	[55]
		NO	-0.14, -0.62		
		N$_2$	-0.40, -0.37		
Graphene	Nb	CO	-0.53	PBE	[63]
		NH$_3$	-0.63		
		CH$_4$	-0.12		
		SO$_2$	-0.32		
		H$_2$S	-1.68		
Graphene	Ag, Pt, Au	NO	-6.91, -6.22, -8.36	PBE	[66]
		NO$_2$	-7.82, -7.38, -9.34		
Graphene	B, N, P, Al	CH$_4$	-0.51, -0.43, -2.13, -3.28	LDA	[57]
Graphene	Ti, N	HCHO	-1.96, -0.22	PBE	[68]
		CO	-0.5, -0.16		
		NO	-1.8, -0.08		
		SO$_2$	-3.34, -0.77		
Graphene	B, N, Al, S	NO	-0.34, -0.09, -1.35, -0.12	PBE	[59]
		NO$_2$	-0.33, -0.26, -2.48, -0.83		
		NH$_3$	-0.02, -0.02, -1.37, -0.003		
		CO	-0.02, -0.01, -0.66, -0.01		
		CO$_2$	-0.01, -0.02, -0.22, -0.004		
		H$_2$O	-0.04, -0.06, -0.81, -0.02		
		SO$_2$	-0.03, -0.19, -1.54, -0.09		
		O$_2$	-0.01, -0.15, -1.66, -0.03		
		H$_2$	-0.014, -0.008, -0.013, -0.006		
		N$_2$	-0.004, -0.017, -0.202, -0.0001		
Graphene	B, N	CO	-0.14, -0.14	CA-PZ	[58]
		NO	-1.07, -0.40		
		NO$_2$	-1.37, -0.98		
		NH$_3$	-0.50, -0.12		
Graphene	P	H$_2$	-0.01	PBE	[67]
		H$_2$O	-0.05		
		CO$_2$	-0.01		
		CO	-0.07		
		N$_2$	-0.009		
		NH$_3$	-0.01		

Many theoretical studies have been conducted on the use of doped graphene as gas sensors. The results evidence that doped graphene sheets are good candidate materials as gas sensors. To experimentally confirm some of the above-mentioned theoretical predictions, various doped graphene materials have been synthesized and evaluated as gas sensors [71-74]. Based on experimental evidence, the sensitivity and selectivity of doped graphene were higher than pristine graphene [71-74]. However, it is difficult to control the doping concentration and the number of graphene layers. Hence, future trends should be focused on the improvement of doped graphene gas sensors through novel, low-cost industrially scalable techniques that allow to control the doping concentration and type in graphene.

5. Conclusions

This review intended to provide an overview of the application of adsorption isotherm models and first-principles studies to graphene gas sensors. By considering the equilibrium data and the adsorption properties of the adsorbent and adsorbate, the adsorption isotherm model can describe the interaction mechanism of the adsorbent and adsorbate at a constant temperature. First-principles studies allow the development of various models to simulate the gas adsorption process and calculate the behaviors of adsorption, including the distance between gas molecules and sensing material, adsorption energy, geometric structure, and charge

transfer analysis to determine the sensitivity of the material. The effect of gas adsorption on the electronic properties of the sensing material can also be calculated. However, theoretical calculations also have some limitations. For example, the actual situation is always more complex than the one envisaged in the ideal model. Some conditions are impossible to simulate at present, such as external light irradiation. This review shows the importance of theoretical studies for designing novel and efficient gas sensors. These theoretical results can help and motivate researchers to design novel and efficient graphene-based gas sensors.

References

1. Kaisti, M., Detection principles of biological and chemical FET sensors. *Biosensors and Bioelectronics* **2017**, *98*, 437-448.

2. Chen, J.; Jang, C.; Xiao, S.; Ishigami, M.; Fuhrer, M. S., Intrinsic and extrinsic performance limits of graphene devices on SiO_2. *Nature Nanotechnology* **2008**, *3*, 206-209.

3. Kong, J.; Franklin, N. R.; Zhou, C.; Chapline, M. G.; Peng, S.; Cho, K.; Dai, H., Nanotube Molecular Wires as Chemical Sensors. *Science* **2000**, 287, 622.

4. Li, J.; Lu, Y.; Ye, Q.; Cinke, M.; Han, J.; Meyyappan, M., Carbon Nanotube Sensors for Gas and Organic Vapor Detection. *Nano Letters* **2003**, 3, 929-933.

5. Liu, X.; Cheng, S.; Liu, H.; Hu, S.; Zhang, D.; Ning, H., A Survey on Gas Sensing Technology. *Sensors* **2012**, *12*, 9635-9665.

6. Meng, Z.; Stolz, R. M.; Mendecki, L.; Mirica, K. A., Electrically-Transduced Chemical Sensors Based on Two-Dimensional Nanomaterials. *Chemical reviews* **2019**, *119*, 478-598.

7. Chen, X.; Wong, C. K. Y.; Yuan, C. A.; Zhang, G., Nanowire-based gas sensors. *Sensors and Actuators B: Chemical* **2013**, *177*, 178-195.

8. Cui, Y.; Wei, Q.; Park, H.; Lieber, C. M., Nanowire Nanosensors for Highly Sensitive and Selective Detection of Biological and Chemical Species. *Science* **2001**, *293*, 1289.

9. Geim, A. K., Graphene: Status and Prospects. *Science* **2009**, *324*, 1530.

10. Novoselov, K. S.; Geim, A. K.; Morozov, S. V.; Jiang, D.; Zhang, Y.; Dubonos, S. V.; Grigorieva, I. V.; Firsov, A. A., Electric Field Effect in Atomically Thin Carbon Films. *Science* **2004**, *306*, 666.

11. Bogue, R., Graphene sensors: a review of recent developments. *Sensor Review* **2014**, *34*, 233-238.

12. Vikrant, K.; Kumar, V.; Kim, K., Graphene materials as a superior platform for advanced sensing strategies against gaseous ammonia. *Journal of Materials Chemistry A* **2018**, *6*, 22391-22410.

13. Schedin, F.; Geim, A. K.; Morozov, S. V.; Hill, E. W.; Blake, P.; Katsnelson, M. I.; Novoselov, K. S., Detection of individual gas molecules adsorbed on graphene. *Nature Materials* **2007**, *6*, 652-655.

14. Tao, W. D. H. Z., A Review on Graphene-Based Gas/Vapor Sensors with Unique Properties and Potential Applications. *Nano-micro letters* **2016**, *8*, 95-119.

15. Huang, L.; Zhang, Z.; Li, Z.; Chen, B.; Ma, X.; Dong, L.; Peng, L., Multifunctional Graphene Sensors for Magnetic and Hydrogen Detection. *ACS Applied Materials & Interfaces* **2015**, *7*, 9581-9588.

16. Hong, J.; Lee, S.; Seo, J.; Pyo, S.; Kim, J.; Lee, T., A Highly Sensitive Hydrogen Sensor with Gas Selectivity Using a PMMA Membrane-Coated Pd Nanoparticle/Single-Layer Graphene Hybrid. *ACS Applied Materials & Interfaces* **2015**, *7*, 3554-3561.

17. Rajesh; Gao, Z.; Charlie Johnson, A. T.; Puri, N.; Mulchandani, A.; Aswal, D. K., Scalable chemical vapor deposited graphene field-effect transistors for bio/chemical assay. *Applied Physics Reviews* **2021**, *8*, 11311.

18. Dua, V.; Surwade, S. P.; Ammu, S.; Agnihotra, S. R.; Jain, S.; Roberts, K. E.; Park, S.; Ruoff, R. S.; Manohar, S. K., All-Organic Vapor Sensor Using Inkjet-Printed Reduced Graphene Oxide. *Angewandte Chemie International Edition* **2010**, *49*, 2154-2157.

19. Lu, G.; Park, S.; Yu, K.; Ruoff, R. S.; Ocola, L. E.; Rosenmann, D.; Chen, J., Toward Practical Gas Sensing with Highly Reduced Graphene Oxide: A New Signal Processing Method To Circumvent Run-to-Run and Device-to-Device Variations. *ACS Nano* **2011**, *5*, 1154-1164.

20. Lemme, M. C.; Echtermeyer, T.; Baus, M.; Szafranek, B. N.; Schmidt, M.; Kurz, H., Towards Graphene Field Effect Transistors. *ECS Transactions* **2019**, *11*, 413-419.

21. Ren, Y.; Zhu, C.; Cai, W.; Li, H.; Ji, H.; Kholmanov, I.; Wu, Y.; Piner, R. D.; Ruoff, R. S., Detection of sulfur dioxide gas with graphene field effect transistor. *Applied Physics Letters* **2012**, *100*, 163114.

22. Colinge, J. P.; Colinge, C. A., *The MOS Transistor.* Springer US: Boston, MA, 2002; p 210.

23. Fu, W.; Jiang, L.; van Geest, E. P.; Lima, L. M. C.; Schneider, G. F., Sensing at the Surface of Graphene Field-Effect Transistors. *Advanced*

Materials **2017**, *29*, 1603610.

24. Bhattacharyya, P., Fabrication Strategies and Measurement Techniques for Performance Improvement of Graphene/Graphene Derivative Based FET Gas Sensor Devices: A Review. *IEEE sensors journal* **2021**, *21*, 10231-10240.

25. Wang, J.; Guo, X., Adsorption isotherm models: Classification, physical meaning, application and solving method. *Chemosphere* **2020**, *258*, 127279.

26. Al-Ghouti, M. A.; Da'Ana, D. A., Guidelines for the use and interpretation of adsorption isotherm models: A review. *Journal of Hazardous Materials* **2020**, *393*, 122383.

27. Langmuir, I., THE ADSORPTION OF GASES ON PLANE SURFACES OF GLASS, MICA AND PLATINUM. *Journal of the American Chemical Society* **1918**, *40*, 1361-1403.

28. Hu, H.; Trejo, M.; Nicho, M. E.; Saniger, J. M.; Garc A-Valenzuela, A., Adsorption kinetics of optochemical NH3 gas sensing with semiconductor polyaniline films. *Sensors and Actuators B: Chemical* **2002**, *82*, 14-23.

29. Gautam, M.; Jayatissa, A. H., Graphene based field effect transistor for the detection of ammonia. *Journal of Applied Physics* **2012**, *112*, 64304.

30. Jaaniso, R.; Kahro, T.; Kozlova, J.; Aarik, J.; Aarik, L.; Alles, H.; Floren, A.; Gerst, A.; Kasikov, A.; Niilisk, A.; Sammelselg, V., Temperature induced inversion of oxygen response in CVD graphene on SiO2. *Sensors and Actuators B: Chemical* **2014**, *190*, 1006-1013.

31. Berholts, A.; Kahro, T.; Floren, A.; Alles, H.; Jaaniso, R., Photo-activated oxygen sensitivity of graphene at room temperature. *Applied Physics Letters* **2014**, *105*, 163111.

32. Crowther, A. C.; Ghassaei, A.; Jung, N.; Brus, L. E., Strong Charge-Transfer Doping of 1 to 10 Layer Graphene by NO2. *ACS Nano* **2012**, *6*, 1865-1875.

33. Wen, C.; Ye, Q.; Zhang, S.; Wu, D., Assessing kinetics of surface adsorption‐desorption of gas molecules via electrical measurements. *Sensors and Actuators B: Chemical* **2016**, *223*, 791-798.

34. Sakamoto, Y.; Uemura, K.; Ikuta, T.; Maehashi, K., Palladium configuration dependence of hydrogen detection sensitivity based on graphene FET for breath analysis. *Japanese Journal of Applied Physics* **2018**, *57*, 4.

35. Phan, D.; Chung, G., A novel nanoporous Pd‐graphene hybrid synthesized by a facile and rapid process for hydrogen detection. *Sensors and Actuators B: Chemical* **2015**, 210, 661-668.

36. Do, D. D., *Adsorption Analysis: Equilibria and Kinetics*. Imperial College Press: London, England, **1998**, *2*, p 916.

37. Gautam, M.; Jayatissa, A. H., Adsorption kinetics of ammonia sensing by graphene films decorated with platinum nanoparticles. *Journal of Applied Physics* **2012**, *111*, 94317.

38. Adamson, A. W.; Gast, A. P., *Physical Chemistry of Surfaces*. 6th ed.; Wiley-Interscience: 1997.

39. Gautam, M.; Jayatissa, A. H., Ammonia gas sensing behavior of graphene surface decorated with gold nanoparticles. *Solid-state electronics* **2012**, *78*, 159-165.

40. Xu, T.; Chen, J.; Yuan, W.; Li, B.; Li, L.; Wu, H.; Zhou, X., Preparation and Hydrogen Storage Characteristics of Surfactant-Modified Graphene. *Polymers (Basel)* **2018**, 10.

41. Myers, D., *Surfaces, Interfaces, and Colloids: Principles and Applications*. 2th ed.; Willy-VCH: New York, USA, 2002; p 179-213.

42. Othman, F. E. C.; Samitsu, S.; Yusof, N.; Ismail, A. F., Effects of carbonization conditions on the microporous structure and high-pressure methane adsorption behavior of glucose-derived graphene. *Korean Journal of Chemical Engineering* **2020**, *37*, 2068-2074.

43. Sterlin Leo Hudson, M.; Raghubanshi, H.; Awasthi, S.; Sadhasivam, T.; Bhatnager, A.; Simizu, S.; Sankar, S. G.; Srivastava, O. N., Hydrogen uptake of reduced graphene oxide and graphene sheets decorated with Fe nanoclusters. *International Journal of Hydrogen Energy* **2014**, *39*, 8311-8320.

44. Kohn, W.; Becke, A. D.; Parr, R. G., Density Functional Theory of Electronic Structure. *The Journal of Physical Chemistry* **1996**, 100, 12974-12980.

45. Zeng, Y.; Lin, S.; Gu, D.; Li, X., Two-Dimensional Nanomaterials for Gas Sensing Applications: The Role of Theoretical Calculations. *Nanomaterials* **2018**, *8*, 851.

46. Tang, X.; Du, A.; Kou, L., Gas sensing and capturing based on two-dimensional layered materials: Overview from theoretical perspective. *WIREs Computational Molecular Science* **2018**, *8*, e1361.

47. Leenaerts, O.; Partoens, B.; Peeters, F. M., Adsorption of H2O, NH3, CO, NO2, and NO on graphene: A first-principles study. *Physical Review B* **2008**, 77.

48. Lin, X.; Ni, J.; Fang, C., Adsorption capacity of H2O, NH3, CO, and NO2 on the pristine graphene. *Journal of Applied Physics* **2013**, *113*, 34306.

49. Wehling, T. O.; Novoselov, K. S.; Morozov, S. V.; Vdovin, E. E.; Katsnelson, M. I.; Geim, A. K.; Lichtenstein, A. I., Molecular Doping of Graphene. *Nano Letters* **2008**, *8*, 173-177.

50. Silvestrelli, P. L.; Ambrosetti, A., Including screening in van der Waals corrected density functional theory calculations: The case of atoms and small molecules physisorbed on graphene. *The Journal of Chemical Physics* **2014**, *140*, 124107.

51. Tang, Y.; Chen, W.; Li, C.; Pan, L.; Dai, X.; Ma, D., Adsorption behavior of Co anchored on graphene sheets toward NO, SO$_2$, NH$_3$, CO and HCN molecules. *Applied Surface Science* **2015**, *342*, 191-199.

52. Rad, A. S.; Abedini, E., Chemisorption of NO on Pt-decorated graphene as modified nanostructure media: A first principles study. *Applied Surface Science* **2016**, *360*, 1041-1046.

53. Shokuhi Rad, A.; Zareyee, D., Adsorption properties of SO$_2$ and O$_3$ molecules on Pt-decorated graphene: A theoretical study. *Vacuum* **2016**, *130*, 113-118.

54. Bo, Z.; Guo, X.; Wei, X.; Yang, H.; Yan, J.; Cen, K., Density functional theory calculations of NO$_2$ and H$_2$S adsorption on the group 10 transition metal (Ni, Pd and Pt) decorated graphene. *Physica E: Low-dimensional Systems and Nanostructures* **2019**, *109*, 156-163.

55. Song, Y.; Wang, L.; Wu, L., Theoretical study of the CO, NO, and N$_2$ adsorptions on Li-decorated graphene and boron-doped graphene. *Canadian Journal of Chemistry* **2017**, *96*, 30-39.

56. Shukri, M. S. M.; Saimin, M. N. S.; Yaakob, M. K.; Yahya, M. Z. A.; Taib, M. F. M., Structural and electronic properties of CO and NO gas molecules on Pd-doped vacancy graphene: A first principles study. *Applied Surface Science* **2019**, *494*, 817-828.

57. Chen, X.; Yang, N.; Ni, J.; Cai, M.; Ye, H.; Wong, C. K. Y.; Leung, S. Y. Y.; Ren, T., Density-Functional Calculation of Methane Adsorption on Graphenes. *IEEE Electron Device Letters* **2015**, *36*, 1366-1368.

58. Zhang, Y.; Chen, Y.; Zhou, K.; Liu, C.; Zeng, J.; Zhang, H.; Peng, Y., Improving gas sensing properties of graphene by introducing dopants and defects: a first-principles study. *Nanotechnology* **2009**, *20*, 185504.

59. Dai, J.; Yuan, J.; Giannozzi, P., Gas adsorption on graphene doped with B, N, Al, and S: A theoretical study. *Applied Physics Letters* **2009**, *95*, 232105.

60. Rungger, I.; Das Pemmaraju, C.; Sanvito, S.; Dolui, K., Possible doping strategies for MoS$_2$ monolayers: An ab initio study. *Physical Review B* **2013**, 88, 75420.

61. Luo, H.; Cao, Y.; Zhou, J.; Feng, J.; Cao, J.; Guo, H., Adsorption of NO$_2$, NH$_3$ on monolayer MoS$_2$ doped with Al, Si, and P: A first-principles study. *Chemical Physics Letters* **2016**, 643, 27-33.

62. Cruz-Martínez, H.; Rojas-Chávez, H.; Montejo-Alvaro, F.; Peña-Castañeda, Y. A.; Matadamas-Ortiz, P. T.; Medina, D. I., Recent Developments in Graphene-Based Toxic Gas Sensors: A Theoretical Overview. *Sensors* **2021**, *21*, 1992.

63. J., K.; H., B. N.; P., K. G., Adsorption of Small Molecules on Niobium Doped Graphene: A Study Based on Density Functional Theory. *IEEE Electron Device Letters* **2018**, *39*, 296-299.

64. Chen, X.; Xu, L.; Liu, L.; Zhao, L.; Chen, C.; Zhang, Y.; Wang, X., Adsorption of formaldehyde molecule on the pristine and transition metal doped graphene: First-principles study. *Applied Surface Science* **2017**, *396*, 1020-1025.

65. Tang, Y.; Liu, Z.; Shen, Z.; Chen, W.; Ma, D.; Dai, X., Adsorption sensitivity of metal atom decorated bilayer graphene toward toxic gas molecules (CO, NO, SO2 and HCN). *Sensors and Actuators B: Chemical* **2017**, *238*, 182-195.

66. Jia, X.; An, L., The adsorption of nitrogen oxides on noble metal-doped graphene: The first-principles study. *Modern Physics Letters B* **2019**, *33*, 1950044.

67. Dai, J.; Yuan, J., Modulating the electronic and magnetic structures of P-doped graphene by molecule doping. *Journal of Physics: Condensed Matter* **2010**, *22*, 225501.

68. Zhang, H.; Luo, X.; Lin, X.; Lu, X.; Leng, Y.; Song, H., Density functional theory calculations on the adsorption of formaldehyde and other harmful gases on pure, Ti-doped, or N-doped graphene sheets. *Applied Surface Science* **2013**, *283*, 559-565.

69. Zhang, H.; Luo, X.; Lin, X.; Zhang, Y.; Tang, P.; Lu, X.; Tang, Y., Band structure of graphene modulated by Ti or N dopants and applications in gas sensing. *Journal of Molecular Graphics and Modelling* **2015**, *61*, 224-230.

70. Shao, L.; Chen, G.; Ye, H.; Wu, Y.; Qiao, Z.; Zhu, Y.; Niu, H., Sulfur dioxide adsorbed on graphene and heteroatom-doped graphene: a first-principles study. *The European Physical Journal B* **2013**, *86*, 54.

71. Guo, L.; Li, T., Sub-ppb and ultra selective nitrogen dioxide sensor based on sulfur doped graphene. *Sensors and Actuators B: Chemical* **2018**, *255*, 2258-2263.

72. Lv, R.; Chen, G.; Li, Q.; McCreary, A.; Botello-Méndez, A.; Morozov, S. V.; Liang, L.; Declerck, X.; Perea-López, N.; Cullen, D. A.; Feng, S.; Elías, A. L.; Cruz-Silva, R.; Fujisawa, K.; Endo, M.; Kang, F.; Charlier, J.; Meunier, V.; Pan, M.; Harutyunyan, A. R.; Novoselov, K. S.; Terrones, M., Ultrasensitive gas detection of large-area boron-doped graphene. *Proceedings of the National Academy of Sciences* **2015**, *112*, 14527.

73. Turner, S.; Yan, W.; Long, H.; Nelson, A. J.; Baker, A.; Lee, J. R. I.; Carraro, C.; Worsley, M. A.; Maboudian, R.; Zettl, A., Boron Doping and Defect Engineering of Graphene Aerogels for Ultrasensitive NO2 Detection. *The Journal of Physical Chemistry C* **2018**, *122*, 20358-20365.

74. Srivastava, S.; Kashyap, P. K.; Singh, V.; Senguttuvan, T. D.; Gupta, B. K., Nitrogen doped high quality CVD grown graphene as a fast responding NO$_2$ gas sensor. *New Journal of Chemistry* **2018**, *42*, 9550-9556.